Hippocampal subfields and their neocortical interactions during autobiographical memory using submillimeter whole-brain fMRI at 7 Tesla

Pitshaporn Leelaarporn[1,2], Marshall A. Dalton[3], Rüdiger Stirnberg[2], Tony Stöcker[2,4], Annika Spottke[2], Anja Schneider[1,2], and Cornelia McCormick[1,2].

1. Department of Neurodegenerative Diseases and Geriatric Psychiatry, University of Bonn Medical Center, Bonn, Germany
2. German Center for Neurodegenerative Diseases, Bonn, Germany
3. School of Psychology, The University of Sydney, Sydney, Australia
4. Department of Physics and Astronomy, University of Bonn, Bonn, Germany

Corresponding author: Cornelia McCormick

Address: University Medical School, Department of Neurodegenerative Diseases and Geriatric Psychiatry, Venusberg-Campus 1 / 53127 Bonn, Germany
Tel.: +49 228 287-31852
Email: Cornelia.McCormick@ukbonn.de

Keywords: autobiographical retrieval, episodic memory, neural networks, functional connectivity

Abstract

Recent advances in ultra-high field 7 Tesla magnet resonance imaging (7T MRI) have provided unprecedented opportunities to gain insights into the brain mechanisms supporting human cognition. The hippocampus, a heterogeneous brain structure comprising several smaller subfields has been firmly established to play a central role during vivid re-experiencing of autobiographical memories (AM). However, due to technical limitations inherent to MRI investigations of the hippocampus, how hippocampal subfields differentially support AM and how hippocampal subfields functionally connect with other brain regions typically associated with AM retrieval remains elusive. To tackle this knowledge gap, we leveraged technical advances of parallel imaging and employed a customized Echo Planar Imaging (EPI) sequence at 0.9 mm isotropic voxel size over the whole brain while participants re-experienced vivid, detail-rich AM. In addition, we developed a processing pipeline that allows the examination of differential activation of hippocampal subfields in single subject space as well as hippocampal-neocortical interactions at a group level. We found that all hippocampal subfields were engaged during AM retrieval but that one specific hippocampal subfield, the pre/parasubiculum, contributed over and above the other subfields to AM retrieval. Moreover, functional connectivity analyses revealed that the pre/parasubiculum was the only hippocampal subfield that strongly connected to other brain regions typically associated with AM, such as ventromedial prefrontal cortex (vmPFC) and medial/lateral parietal regions. Our results support recent proposals that the pre/parasubiculum may play an essential role in cognitive tasks that rely heavily on visual imagery, such as the vivid re-experience of personal past events.

Introduction

Neuropsychological and functional magnetic resonance imaging (fMRI) studies have firmly established that vivid autobiographical memories (AM, i.e., memories of personal past events) are supported by the hippocampus as a central structure within a broader brain network comprising the ventromedial prefrontal cortex (vmPFC) and medial/lateral parietal cortices (1–6). However, the hippocampus is a heterogeneous brain structure comprising several subfields including the dentate gyrus (DG), Cornu Ammonis (CA) 1-4, subiculum, presubiculum, and parasubiculum. There is a dearth of information regarding how the activity of these hippocampal subfields may differ during AM retrieval as well as how the subfields interact with other neocortical regions in the broader neocortical AM network.

This knowledge gap exists primarily due to technical limitations inherent to traditional 3 Tesla (3T) fMRI (7) investigations. Traditional 3T fMRI sequences at a whole-brain level and a reasonable repetition time are usually limited to a voxel size of approximately 3 mm isotropic, thus prohibiting imaging of small brain structures like hippocampal subfields in a whole-brain setting. Technical advances in high-resolution 3T fMRI have facilitated an increase in spatial resolution that can be used to capture dissociable activity of small adjacent brain structures of the medial temporal lobes, including hippocampal subfields (8–10). However, these sequences require a reduced field-of-view for a reasonable temporal resolution, thus precluding a whole-brain functional scan. Recent innovations in ultra-high field 7 Tesla (7T) fMRI sequence development including 2D high parallel imaging acceleration capabilities allow, for the first time, to scan at a submillimeter voxel size at a whole-brain level. This enables us to conduct more detailed examinations of functional interactions between hippocampal subfields and the neocortex during a cognitive task (11, 12).

To date, few studies have investigated memory signals using 7T fMRI (13–15). For example, recent reduced field-of-view 7T fMRI studies examined hippocampal subfield contributions to distinguish

between or combine similar experiences (14, 15). Other neuroimaging studies have exploited advances of 7T fMRI to study targeted layer-specific effects of mnemonic processes (16–18). However, to our knowledge, no study has hitherto leveraged both increased speed and spatial resolution of 7T fMRI to examine differential hippocampal subfield – neocortical interactions during AM retrieval.

AM retrieval is a complex cognitive task relying on multiple processes and entails the construction of a coherent detail-rich mental event in the mind's eye (19, 20). Notably, vivid mental imagery has recently been linked to the rich re-experience of AM retrieval (21–23). Thus far, reduced field-of-view 3T fMRI studies have indicated that a specific region of the medial hippocampus, aligning with the location of the presubiculum and parasubiculum (hereafter referred to collectively as the pre/parasubiculum), may be a crucial hub for the mental construction of internal models of scenes and may provide the visuospatial building blocks of AM retrieval (24). Specifically, the pre/parasubiculum shows greater activation during mental construction of mental models couched in a 3-dimensional visuospatial framework (scene) over more abstract mental models couched in a 2-dimensional visuospatial framework (25). From a neuroanatomical perspective, the pre/parasubiculum has strong direct connections to numerous cortical brain regions which bypass entorhinal-mediated pathways (26). One idea is that the pre/parasubiculum lies at the apex of specific visuospatial processing pathways and may integrate information into coherent scene imagery in the mind's eye (24, 27). Within this framework, pre/parasubiculum dependent scene imagery could well be the spatial stage upon which AM are recollected. In line with this proposal, volumes of the subiculum and pre/parasubiculum show strong correlations with specific details recalled during AM (28, 29). Thus, a hypothesis tested in the current study is that the

pre/parasubiculum may be more involved in vivid, detail-rich AM retrieval than other hippocampal subfields.

In further support of the proposal that the pre/parasubiculum plays an important role in AM, numerous whole-brain 3T fMRI studies (although not explicitly looking at hippocampal subfields due to limitations in spatial resolution) consistently observe activity in the medial hippocampus aligning with the location of the pre/parasubiculum during AM retrieval (see Zeidman et al. (30) for review). In addition, previous research has shown that a region of the anterior medial body of the hippocampus (aligning with the location of the pre/parasubiculum) was functionally connected with the vmPFC and medial/lateral parietal cortices during the vivid re-experiencing of autobiographical memories (5). Therefore, we hypothesized that the pre/parasubiculum would show stronger activity during AM than other hippocampal subfields and that the pre/parasubiculum would be functionally connected to other brain regions of the AM network.

Results

Behavioural Results

24 participants were included in the current study and all were able to recall detail-rich autobiographical memories (average of 1.92 ± 0.67, where 1 described the ability to recall detail-rich memories and 6 described the inability to recall any personal events) and construct vivid mental images (average of 1.83 ± 0.69, where 1 referred to the ability create detail-rich mental images and 6 referred to the lack of visual imagery). During scanning, participants were presented with 40 AM cues (e.g., a party) and 40 simple math (MA) problems (e.g., 13 + 53) and were asked to retrieve a personal event specific in time and place or solve the MA problem. Once they retrieved a memory or solved the MA problem, participants were asked to press a button and either elaborate on the memory or add 3's to the MA solution iteratively. Overall, the participants spent 3.53 s (± 0.98) on average to select a memory and around 3.66 s (± 0.97) to solve the MA problem. Whereas some trials were excluded from the analyses due to missing button presses, no significant difference was

found between the speed of AM retrieval and MA solving ($t = 0.8601$, $p = 0.3958$). Participants indicated in 35.67 (± 4.67) trials out of 40 trials that their memories were vivid ($t = 19.36$, $df = 23$, $p < 0.0001$) and 28.13 (± 6.15) trials out of 40 MA problems were reported as easy ($t = 8.553$, $df = 23$, $p < 0.0001$).

Hippocampal Subfield Activation During AM

To preserve maximum spatial precision of the small and complex shapes of hippocampal subfields, hippocampal subfield fMRI analyses were performed in native space with minimal smoothing (see Materials and Methods for more details on preprocessing). Greater bilateral hippocampal activation during AM retrieval than MA solving was found in all participants (see Figure 1 for representative single subject activation). To examine differential activation of hippocampal subfields, all hippocampi were manually segmented from the T2-weighted images into DG/CA4, CA2/3, CA1, subiculum, and the pre/parasubiculum following a standard procedure (31) (see Figure 1 for a representative reconstruction of the segmented hippocampus). The individual masks of the segmented hippocampal subfields were used as regions of interest (ROIs) to extract fMRI signal intensities for each participant during the AM retrieval task and the MA task. Since we found no laterality effect in the whole hippocampus ($t = 1.04$, $df = 23$, $p = 0.3568$) or in any of the hippocampal subfields (see Table S1), we collapsed activity measures of the left and right hemisphere in the following analysis,

All hippocampal subfields showed greater activation during AM retrieval than solving a MA problem (DG/CA4: $t = 6.140$, $df = 23$, $p < 0.001$, CA2/3: $t = 5.217$, $df = 23$, $p < 0.001$, CA1: $t = 3.768$, $df = 23$, $p = 0.001$, subiculum: $t = 3.068$, $df = 23$, $p = 0.005$, pre/parasubiculum: $t = 4.637$, $df = 23$, $p < 0.001$, Bonferroni corrected). To assess differential hippocampal subfield activation, the difference between signal intensities during AM and MA was calculated for each subfield in each participant and assessed using a one-way repeated measures ANOVA with Tukey's multiple comparisons test ($F = 5.887$, $df = 5$, $p = 0.017$, Figure 1 and Table S1 for an overview of % signal changes). In line with our hypothesis, we found that activation relating to AM was much stronger in the

pre/parasubiculum than in CA1 (df = 23, p = 0.001), the subiculum (df = 23, p = 0.001), CA2/3 (df = 23, p = 0.049), and at a trend level in DG/CA4 (df = 23, p = 0.075).

Besides the anatomically defined hippocampal subfields, much debate involves different functions of those subfields along the long-axis of the hippocampus (30). Specifically, the anterior medial hippocampus seems to be a hot spot for scene-based cognition (24, 25, 30). Furthermore, a recent study has revealed that this specific part of the hippocampus displays a high degree of anatomical connectivity with visuospatial processing areas in temporal, medial parietal and occipital cortices in the human brain (26). Thus, in an additional analysis, we split individual subfield masks along the long-axis of the hippocampus into sections (i.e., anterior, anterior body, posterior body and tail) and repeated the previous analysis for the subfields in the anterior body section (see Figure S2). The main RM-ANOVA found differences within activation levels of the subfields within the anterior body portion (F = 4.440, df = 4, p = 0.024). The activation relating to AM versus MA was much stronger in the anterior body of the pre/parasubiculum than in CA1 (df = 23, p < 0.001), CA2/3 (df = 23, p = 0.019), subiculum (df = 23, p = 0.034), and DG/CA4 (df = 23, p = 0.034).

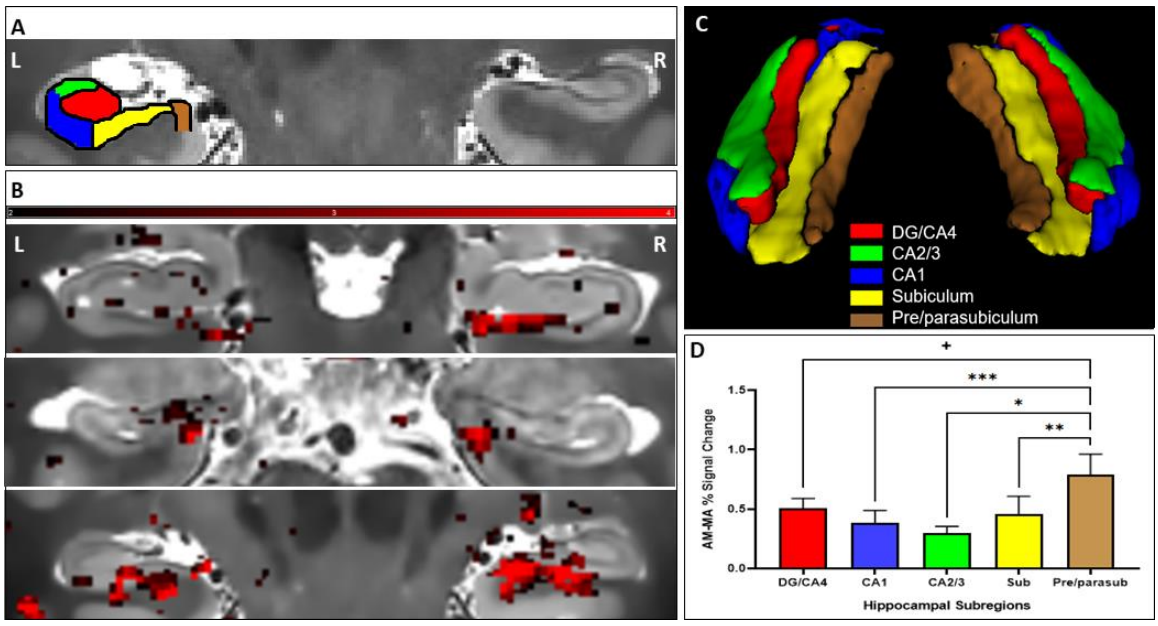

Figure 1. A. Overlaid segmentation of labelled hippocampal subfields, including the DG, CA1-4, subiculum, and pre/parasubiculum on high-resolution structural T2-weighted scan. B. Examples of

AM versus MA activation (shown in red) from three participants. C. An example of manual hippocampal subfield segmentation (note the uncal portion of the hippocampus was not analysed in this study; see methods). D. The comparison between the % signal change during AM and MA in hippocampal subfields (DG/CA4, CA1, CA2/3, subiculum, and pre/parasubiculum). *** $p < 0.001$, ** $p < 0.01$, and * $p < 0.05$, and + $p < 0.01$ (non-significant trend level). The pre/parasubiculum showed stronger differentiation between AM and MA than most other subfields.

Hippocampal Subfield - Neocortical Interactions During AM

In order to assess whole-brain activation correlating with AM retrieval, we conducted a multivariate partial least squares (PLS) analysis (see Materials and Methods for more information on PLS). Aligning with previous 3T fMRI studies (2, 5), we found greater activation during AM retrieval than MA in all regions typically associated with AM retrieval, including bilateral hippocampal activation as well as vmPFC and medial/lateral parietal activation (LV1, $p < 0.0001$, see Figure 2 and Table S3 for peak MNI coordinates).

To evaluate patterns of whole-brain functional connectivity of hippocampal subfields at a group level, we conducted multivariate seed PLS analyses. This technique allowed us to use the individual activations of hippocampal subfields (obtained in native space) as seeds in a group analysis based on fMRI data which were now normalized. Furthermore, seed PLS enabled us to establish, at a whole-brain level, whether functional connectivity of specific hippocampal subfields differed between AM and MA. In an overarching seed PLS, we found that hippocampal subfield connectivity differentiated between AM and MA (LV 1, $p = 0.039$). In Bonferroni corrected post hoc analyses (thus applying a threshold of $p < 0.01$), we found that only the functional connectivity of the pre/parasubiculum differed between both conditions (pre/parasubiculum: $p = 0.0001$), whereas the other subfields did not survive this threshold (DG/CA4: $p = 0.53$, CA2/3: $p = 0.06$, CA1: $p = 0.15$, subiculum: $p = 0.18$). Figure 2 illustrates the brain pattern associated with functional connectivity of the pre/parasubiculum during AM, including all canonical regions typically associated with this cognitive task, including the vmPFC and medial/lateral parietal cortices (see

Table S4 for peak MNI coordinates). In addition, the pre/parasubiculum was stronger functionally connected to posterior visual-perceptual cortices during AM than MA.

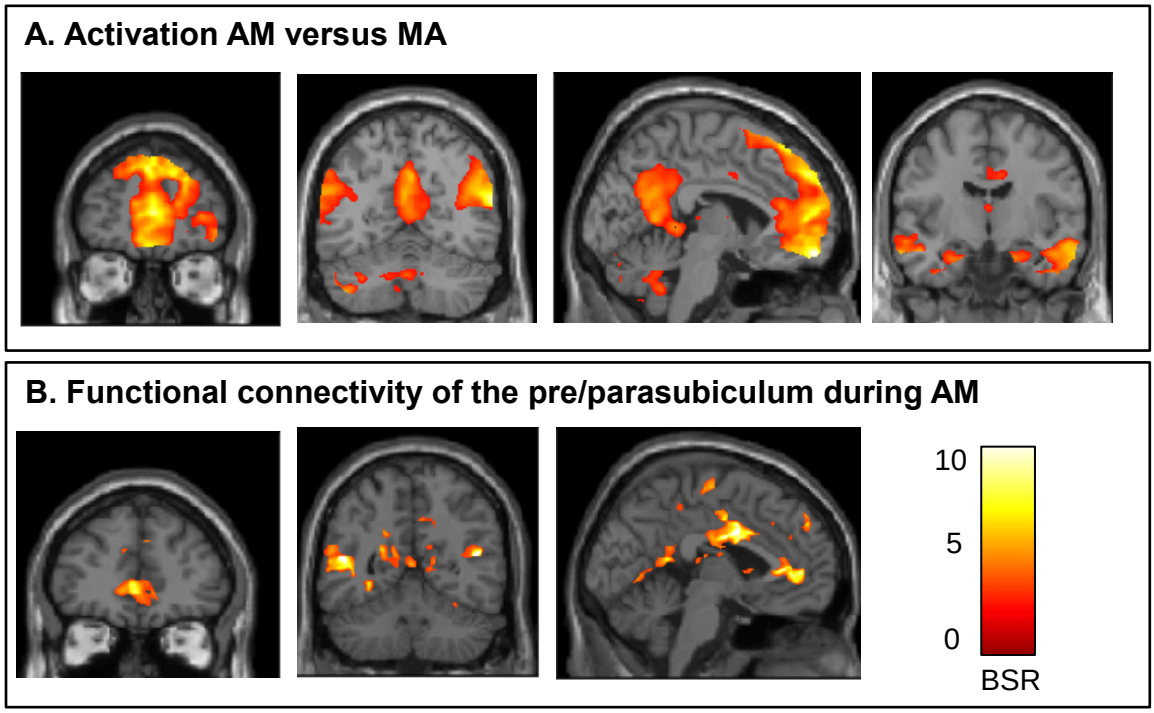

Figure 2. A. Greater activation for AM versus MA is shown in bootstraps ratios (BSR). All regions typically associated with AM show greater activation of bilateral hippocampi, vmPFC and medial/lateral parietal cortex for AM. The whole-brain fMRI activation is overlaid on a standard T1-weighted MRI image. B. Greater functional connectivity of the pre/parasubiculum during AM than MA is shown. All regions typically associated with AM retrieval show strong functional connectivity, including vmPFC and medial/lateral parietal cortices.

Discussion

By exploiting ultra-high resolution 7T fMRI, this study provides two novel insights into hippocampal memory processes. First, we found evidence that the pre/parasubiculum was more engaged during the vivid re-experience of AMs than neighboring hippocampal subfields. Second, during AM, the pre/parasubiculum was strongly functionally connected to neocortical brain regions typically engaged during AM retrieval such as vmPFC and medial/lateral parietal cortices. We discuss these findings in turn.

We observed that all hippocampal subfields differentiated between AM and MA with the pre/parasubiculum differentiating both cognitive tasks to a greater extent than the neighboring subiculum and the CA1 fields. This indicates that our study design specifically engaged the pre/parasubiculum. Examining our study design closer, we only included participants who reported to be able to retrieve visually detail-rich AMs easily and we focused our analyses on the last 8 secs of the AM trials, thus highlighting the period in which participants were mostly engaged in re-experiencing visual-perceptual imagery. This suggests that our results align with recent proposals that the pre/parasubiculum is preferentially engaged in tasks which rely on vivid scene-based cognition (24). For example, the pre/parasubiculum showed stronger activation for scene-imagery than object-imagery (25, 32), and scene/object discrimination (33). Furthermore, we know from rodents and nonhuman primates that the pre/parasubiculum contains an abundance of head, grid, and border cells (34, 35), which has recently been extended to human goal direction cells (36). Arguably, AM retrieval relies heavily on scene-based cognition since AMs tend to unfold on a visuo-spatial stage (21). In fact, when participants are asked to conjure up personal events, they tend to place the event onto a spatial stage (22), indicating that visuo-spatial imagery plays a fundamental role in episodic memory retrieval. Further strengthening the tight link between the ability to recall AMs and visual imagery, people with little or no ability to experience visual imagery, so called aphantasics, also tend to have difficulties recalling AM (23, 37–39). Interestingly, aphantasics not only have difficulties to recall visual-perceptual details to their AMs, but they seem to have a worse ability to retrieve personal memories in general (37) and show poorer verbal and non-verbal memory function (40). In fact, a recent phenomenon called severe deficient autobiographical memory or SDAM (41, 42) has also been associated with aphantasia (43). This line of thought meshes well with the scene construction theory positing that a dominant function of the hippocampus is to construct spatially coherent internal models of the environment (24, 30, 44, 45), and the pre/parasubiculum may be of special significance to this process (24, 25). In line with the scene construction theory, patients with hippocampal damage have been shown to use less scene-based cognition in their mind-wandering episodes (46), moral decision-making (47), and scene-

based judgements (48). Therefore, our results point towards a crucial role of the pre/parasubiculum in tasks relying heavily on vivid visuo-spatial imagery, such as vivid AM retrieval.

Having highlighted the role of the pre/parasubiculum in vivid AM retrieval, we further found that all other hippocampal subfields also showed stronger activation during AM retrieval than MA. Since AM retrieval is a complex cognitive task with a magnitude of different operations (such as detail integration, and discrimination), it is likely that the other hippocampal subfields contribute to different processes which we did not try to dissociate in the current study. In fact, recent investigations show different contributions of hippocampal subfields to mnemonic processes. Although there is somewhat mixed evidence, CA fields tend to be implicated in the integration or associations of memory details (15, 49, 50), whereas the DG (14, 50–52) tend to support the separation or discrimination of mnemonic information. Our newly developed 7T fMRI sequence will allow the innovative investigation of differential hippocampal subfield contributions to cognition.

A major goal of the current study was to examine functional connectivity of hippocampal subfields to the neocortex during AM retrieval. We found that the pre/parasubiculum has strong functional connectivity to neocortical regions known to support AM retrieval. This finding is supported by several lines of research. For example, both 3T and 7T fMRI resting state studies identified the subiculum (in which the pre/parasubiculum was included) as a functional connectivity hub correlating with activity in the default mode network which has overlapping brain regions to the AM network (53, 54). In addition, previous task-based 3T fMRI revealed that hippocampal functional connectivity during AM of a seed region in the vicinity of the pre/parasubiculum (5) was strongly connected to a brain-wide network comprising the vmPFC and medial/lateral parietal cortices, as well as visual-perceptual regions of the occipital cortex. Furthermore, the same region of the anterior medial hippocampus was more strongly connected to frontal and parietal cortices during scene construction than object construction (32). Additionally, from a neuroanatomical perspective, the pre/parasubiculum presents a primary target of the parieto-medial temporal visual pathway

carrying information about visuospatial representations of the environment (24). The parieto-medial temporal pathway directly links the pre/parasubiculum with the inferior parietal lobule, posterior cingulate cortex, retrosplenial cortex, and parahippocampal gyrus (27, 55). Each of these regions have been heavily associated with visuospatial cognition (56, 57) and AM (58) and each have direct anatomical connections with the pre/parasubiculum, giving it privileged access to visuo-spatial information. While most of this evidence stems from anatomical connectivity studies in rodent and nonhuman primates, a recent diffusion imaging study supports this framework by showing that circumscribed regions of the human pre/parasubiculum have dense patterns of anatomical connectivity with distributed cortical brain areas (26).

In sum, here we utilized a novel rapid, submillimeter 7T fMRI sequence which enabled us to examine functional connectivity between hippocampal subfields and neocortical regions during vivid AM retrieval. We enhanced our knowledge of hippocampal subfield contributions to cognition by showing that the pre/parasubiculum was more engaged during AM than other neighboring hippocampal subfields and that the pre/parasubiculum was strongly functionally connected to regions typically recruited during AM. By focusing on visuo-spatial aspects of AM retrieval, our results indicate a prime role of the pre/parasubiculum in scene-based cognition.

Materials and Methods

Participants

24 healthy young individuals (right-handed, age: 26.66 ± 4.15 years old, Males: 12, Females: 12) with no history of neurological or psychiatric disorders with either normal or corrected-to-normal vision were recruited. In order to examine vivid, detail-rich AM retrieval, we only included people that were able to recall detail-rich personal memories and construct mental images with ease. All participants provided oral and written informed consent in accordance with the local ethics board.

Autobiographical Memory and Visual Imagery Assessment

Participants were asked to assess their ability to recall vivid AMs on a Likert scale from 1 to 6 where 1 described the ability to recall detail-rich memories and 6 described the inability to recall any personal events. Furthermore, participants were asked to assess their ability to construct vivid mental images on a Likert scale from 1 to 6 where 1 referred to the ability create detail-rich mental images and 6 referred to the lack of visual imagery. This procedure was adapted from Clark et al (59).

Experimental fMRI Task

The experimental task was adapted from a previous protocol by McCormick et al. (5). The experimental procedure was clarified to the participants prior to the scanning. Participants were presented with a set of 40 randomized trials consisting of an AM retrieval task and a simple MA task as a baseline. Each trial lasted a maximum of 17 s with a jittered inter-stimulus interval (ISI) between 1 - 4 s. The AM trials consisted of word cues of various general events, e.g., birthday celebration. Participants were instructed to search for a relevant personal event which was specific in time and place and more than one year ago and press a response button once a memory had been chosen. Participants were then asked to re-experience the memory in their mind by re-living the event with as many perceptual details as possible. In comparison, the MA trials consisted of simple addition or subtraction problems, e.g., 13 + 53. After the MA problem was solved, participants were instructed to press a response button and add 3 to the solution iteratively, e.g., (13 + 53) + 3 + 3n. Following all AM trials, participants were asked to indicate with a button press whether the AM had been re-experienced in a detailed manner or whether the retrieval was faint. Following all MA trials, participants were asked to indicate with a button press whether the MA problem had been easy or difficult.

MRI Data Acquisition

MRI data were acquired using a MAGNETOM 7T Plus ultra-high field scanner (Siemens Healthineers, Erlangen, Germany). Participants viewed the stimulus screen placed at the back end of the scanner bore through a mirror mounted between the inner 32 channel receive head coil and the outer circular polarized transmit coil. The MRI protocol consisted of the following scans:

Whole-brain T1-weighted structural image: A 0.6 mm isotropic whole-brain T1-weighted multi-echo MP-RAGE scan was acquired using a custom sequence optimized for scanning efficiency (60) and minimal geometric distortions (61) (TI = 1.1 s, TR = 2.5 s, TEs = 1.84/3.55/5.26/6.92 ms, FA = 7°, TA = 7:12, readout pixel bandwidth: 970 Hz, matrix size: 428 x 364 x 256, elliptical sampling, sagittal slice orientation, CAIPIRINHA (62) $1x2_{z1}$ parallel imaging undersampling with on-line 2D GRAPPA reconstruction, turbofactor: 218). Finally, the four echo time images were collapsed into a single high-SNR image using root-mean-squares combination.

Reduced hippocampus field-of-view T2-weighted structural image: For motion-robust hippocampal subfield-segmentation, three rapid, 0.4 mm x 0.4 mm x 1.0 mm T2-weighted, slice-selective TSE scans were acquired consecutively on a reduced hippocampus field-of-view (TE = 76 ms, TR = 8090 ms, FA = 60° using Hyperecho (63), TA = 2:59, readout pixel bandwidth: 150 Hz, matrix size: 512 x 512, 55 oblique-coronal slices of 1 mm thickness orthogonal to the long hippocampus axis, 3-fold parallel imaging undersampling with online 1D GRAPPA reconstruction, turbofactor: 9). The RF transmit power reference voltage was varied across the scans (200V, 240V, 280V) such that the nominal refocusing flip angles of the protocol were approximately reached in all brain regions in at least one of the scans. Finally, the three images from each participant were coregistered, denoised following the Rician noise estimation (64) and averaged.

Rapid whole-brain ultra-high spatial resolution fMRI: For rapid whole-brain fMRI at submillimeter resolution, a custom interleaved multishot 3D echo planar imaging (EPI) sequence

was used (12) (TE = 21.6 ms, TR_{vol} = 3.4 s, FA = 15°, 6/8 partial Fourier sampling along the primary phase encode direction, oblique-axial slice orientation along the anterior-posterior commissure line, readout pixel bandwidth: 1136 Hz, matrix size: 220 x 220 x 140). To obtain both a high nominal spatial resolution of 0.9 mm isotropic and a reasonably high temporal resolution of TR_{vol} = 3.4 s whilst imaging the whole brain at sufficient signal-to-noise-ratio (SNR) with a BOLD-optimal TE, several unique sequence features were combined for the first time at 7T. A: skipped-CAIPI $3.1x7_{z2}$ parallel imaging undersampling (SNR-optimized 7-fold CAIPIRINHA undersampling pattern combined with interleaved 3-shot segmentation) (12) with on-line 2D GRAPPA reconstruction. B: one externally acquired phase correction (navigator) scan per volume instead of typical integrated three navigator echoes per shot (12). C: semi-elliptical sampling (variable echo train lengths) skipping only the latest EPI echoes outside of an elliptical k-space mask that defines 0.9 mm isotropic voxel resolution (11). D: Rapid slab-selective binomial-121 water excitation instead of time-consuming fat saturation (65). A 3-minute fMRI practice-run was performed before the two main sessions, each lasting for 15 min. The MRI scan session was concluded by a standard 3 mm isotropic two-echo gradient-echo field-mapping scan acquired within 35 s.

MRI Data Processing

Segmentation of Hippocampal Subfields: Manual segmentation of hippocampal subfields was performed on the averaged and denoised native space T2-weighted structural scans according to the protocol described by Dalton and colleagues (31). ROI masks were created for six hippocampal subfields including DG/CA4, CA3/2, CA1, subiculum, pre/parasubiculum, and uncus using the software application ITK-SNAP 3.8 (66). We excluded the uncus from our analyses because this region contains a mix of different hippocampal subfields (67) that are difficult to differentiate on structural MRI scans (31) even with the high-resolution achieved in the current study. To assess intra- and inter-rater reliability, five hippocampi were segmented by two independent raters (P.L. and M.A.D) and again six months after initial segmentation. The inter-rater reliability as measured by the DICE overlap metric (68) were in accordance with those reported in the extant literature (69,

70) (0.87 for DG/CA4, 0.73 for CA3/2, 0.80 for CA1, 0.80 for subiculum, and 0.64 for pre/parasubiculum). Intra-rater reliability was measured 8 months apart and also showed high concordance between segmentations at the two different time points (0.92 for DG/CA4, 0.79 for CA3/2, 0.84 for CA1, 0.84 for subiculum, and 0.86 for pre/parasubiculum).

Functional MRI preprocessing: To address both research aims, two steps of MRI preprocessing were performed using SPM12 (Statistical Parametric Mapping 12) software package (www.fil.ion.ucl.ac.uk/spm/) on MATLAB v17a (MathWorks) computing platform (https://matlab.mathworks.com/). For both steps, the anatomical and the functional scans obtained from each subject were reoriented to be in line with the anterior-posterior commissure axis. The field maps, including the phase and magnitude images, were used to calculate the voxel displacement maps (VDM) to geometrically correct the distorted EPI images. The VDMs were then applied to the functional scans during realignment and unwarping. The averaged anatomical scans (and hippocampal subfield masks) were co-registered with the functional scans. For the first aim (to examine differential activation of hippocampal subfields), fMRI data were kept in native space to allow maximum spatial precision. Here, a Gaussian smoothing kernel of the native functional scans were set to 1 mm full-width half-maximum (FWHM). The temporal high-pass filter was set to 128 s. One-sample T-Test contrasts (T-contrasts) were selected to test the effects AM retrieval versus baseline (MA). For the second aim (to examine functional connectivity of hippocampal subfields to other neocortical regions), motion-corrected fMRI data were normalized to the Montreal Neurological Institute (MNI) space and smoothed with 6 mm FWHM to examine activation and functional connectivity at the group level.

Statistical Analyses

Hippocampal Subfield Activation Extraction: Signal intensity values for AM and MA of five hippocampal subfield ROIs were extracted for each participant for each hemisphere in native space using MATLAB-based Response Exploration (REX) toolbox (https://www.nitrc.org/projects/rex).

Since we found no evidence of laterality effects, signal intensities for both hemispheres were collapsed. Differences in signal intensity during AM and MA for hippocampal subfields were compared using Student's T-Tests with Bonferroni correction, so that a significant threshold of $p < 0.01$ was applied. Furthermore, to assess differential activation between hippocampal subfields, the difference between signal intensities relating to AM and MA was calculated for each subfield and the resulting values were subjected to a 1-way-RM-ANOVA with Tukey's multiple comparison test. A significance threshold of $p < 0.05$ was applied.

Group analyses of whole brain activation and hippocampal subfield functional connectivity

First, to assess differences between AM and MA, a multivariate mean-centered partial least squares (PLS) group analysis was performed. Detailed descriptions of PLS can be found elsewhere (71, 72). In brief, PLS uses singular value decomposition to extract ranked latent variables (LVs) from the covariance matrix of brain activity and conditions in a data driven manner. These LVs express patterns of brain activity associated with each condition. Statistical significance of the LVs was assessed using permutation testing. In this procedure, each participant's data was randomly reassigned (without replacement) to different experimental conditions, and a null distribution was derived from 500 permutated solutions. We considered LVs as significant at $p < 0.05$. Furthermore, we assessed the reliability of each voxel that contributed to a specific LV's activity pattern using a bootstrapped estimation of the standard error (bootstrap ratio, BSR). For each bootstrapped solution (100 in total), participants were sampled randomly with replacement and a new analysis was performed. In the current study, we considered clusters of 50 or more voxels with BSRs greater than 3 (approximately equal to a $p < 0.001$) to represent reliable patterns of activation. Of note, PLS uses two re-sampling techniques that (1) scramble the data of each participant's conditions so that small but reliable differences between true experimental conditions can be detected, and (2) exclude whole datasets of participants, so that outliers who may drive significant effects can be detected.

To assess functional connectivity between hippocampal subfields and the rest of the brain, seed PLS, an extension of the mean-centered PLS was used (72). Signal intensities of individual subfields (extracted in native space) were used as seeds for the group analyses (performed in MNI space). At first, signal intensities of all five hippocampal subfields were included in an overall seed PLS to establish whether hippocampal subfield connectivity would differ during AM retrieval and MA solving. A significance threshold for the LV's (500 permutations) of $p < 0.05$ was applied. In post hoc analyses, functional connectivity of each of the five hippocampal subfields were assessed separately and a Bonferroni multiple comparison correction was applied so that we considered statistical significance for the LV's at $p < 0.01$ (see for a similar approach (73)). Boot strap ratios (100 bootstraps) of < 2.5 and > -2.5 (corresponding approximately to a $p < 0.01$) were considered significant.

Acknowledgments

CMC and PL are supported by a BONFOR fellowship (2019-2-06,2021-2A-01). We thank Sascha Brunheim, Anke Rühling and Jennifer Schlee for their technical support during scanning and all participants for their time.

References

1. W.B. Scoville, B. Milner, Loss of recent memory after bilateral hippocampal lesions. *J. Neurol. Neurosurg. Psychiatry* **20**, 11–21 (1957).
2. M. Moscovitch, *et al.*, Functional neuroanatomy of remote episodic, semantic and spatial memory: a unified account based on multiple trace theory. *J. Anat.* **207**, 35–66 (2005).
3. D. R. Addis, A. T. Wong, D. L. Schacter, Remembering the past and imagining the future: common and distinct neural substrates during event construction and elaboration. Neuropsychologia 45, 1363–1377 (2007).
4. R.S. Rosenbaum, *et al.*, Patterns of autobiographical memory loss in medial-temporal lobe amnesic patients. *J. Cogn. Neurosci.* **20**, 1490–1506 (2008).
5. C. McCormick, M. St-Laurent, A. Ty, T.A. Valiante, M.P. McAndrews, Functional and effective hippocampal-neocortical connectivity during construction and elaboration of autobiographical memory retrieval. *Cereb. Cortex* **25**, 1297–1305 (2015).
6. C. McCormick, D.N. Barry, A. Jafarian, G.R. Barnes, E.A. Maguire, vmPFC Drives Hippocampal Processing during Autobiographical Memory Recall Regardless of Remoteness. *Cereb. Cortex* **30**, 5972–5987 (2020).
7. T. Willems, K. Henke, Imaging human engrams using 7 Tesla magnetic resonance imaging. *Hippocampus* **31**, 1257–1270 (2021).
8. M.A. Dalton, C. McCormick, F. De Luca, I.A. Clark, E.A. Maguire, Functional connectivity along the anterior-posterior axis of hippocampal subfields in the ageing human brain. *Hippocampus* **29**, 1049–1062 (2019).
9. M.A. Dalton, C. McCormick, E.A. Maguire, Differences in functional connectivity along the anterior-posterior axis of human hippocampal subfields. *Neuroimage* **192**, 38–51 (2019).
10. H.M. Bonnici, *et al.*, Detecting representations of recent and remote autobiographical memories in vmPFC and hippocampus. *J. Neurosci.* **32**, 16982–16991 (2012).

11. R. Stirnberg, *et al.*, Rapid whole-brain resting-state fMRI at 3 T: Efficiency-optimized three-dimensional EPI versus repetition time-matched simultaneous-multi-slice EPI. *Neuroimage* **163**, 81–92 (2017).

12. R. Stirnberg, T. Stöcker, Segmented K-space blipped-controlled aliasing in parallel imaging for high spatiotemporal resolution EPI. *Magn. Reson. Med.* **85**, 1540–1551 (2021).

13. U.M. Risius, *et al.*, Retrieval, monitoring, and control processes: a 7 tesla FMRI approach to memory accuracy. *Front. Behav. Neurosci.* **7**, 24 (2013).

14. D. Berron, *et al.*, Strong evidence for pattern separation in human dentate gyrus. *J. Neurosci.* **36**, 7569–7579 (2016).

15. X. Grande, *et al.*, Holistic recollection via pattern completion involves hippocampal subfield CA3. *J. Neurosci.* **39**, 8100–8111 (2019).

16. A. Maass, *et al.*, Laminar activity in the hippocampus and entorhinal cortex related to novelty and episodic encoding. *Nat. Commun.* **5**, 5547 (2014).

17. D.G. Norris, J.R. Polimeni, Laminar (f)MRI: A short history and future prospects. *Neuroimage* **197**, 643–649 (2019).

18. E.S. Finn, L. Huber, D.C. Jangraw, P.J. Molfese, P.A. Bandettini, Layer-dependent activity in human prefrontal cortex during working memory. *Nat. Neurosci.* **22**, 1687–1695 (2019).

19. M.A. Conway, C.W. Pleydell-Pearce, The construction of autobiographical memories in the self-memory system. *Psychol. Rev.* **107**, 261–288 (2000).

20. M.A. Conway, Episodic memories. *Neuropsychologia* **47**, 2305–2313 (2009).

21. D.L. Greenberg, B.J. Knowlton, The role of visual imagery in autobiographical memory. *Mem. Cognit.* **42**, 922–934 (2014).

22. J. Robin, B.R. Buchsbaum, M. Moscovitch, The primacy of spatial context in the neural representation of events. *J. Neurosci.* **38**, 2755–2765 (2018).

23. F. Milton, *et al.*, Behavioral and Neural Signatures of Visual Imagery Vividness Extremes: Aphantasia versus Hyperphantasia. *Cereb. Cortex Commun.* **2**, tgab035 (2021).

24. M.A. Dalton, E.A. Maguire, The pre/parasubiculum: a hippocampal hub for scene-based cognition? *Curr. Opin. Behav. Sci.* **17**, 34–40 (2017).

25. M.A. Dalton, P. Zeidman, C. McCormick, E.A. Maguire, Differentiable Processing of Objects, Associations, and Scenes within the Hippocampus. *J. Neurosci.* **38**, 8146–8159 (2018).

26. M.A. Dalton, A. D'Souza, J. Lv, F. Calamante, Anatomical connectivity along the anterior-posterior axis of the human hippocampus: new insights using quantitative fibre-tracking. *BioRxiv* doi: 10.1101/2021.11.17.469032 (2021) doi:10.1101/2021.11.17.469032.

27. D. J. Kravitz, K. S. Saleem, C. I. Baker, M. Mishkin, A new neural framework for visuospatial processing. Nat. Rev. Neurosci. 12, 217–230 (2011).

28. D.J. Palombo, *et al.*, Episodic autobiographical memory is associated with variation in the size of hippocampal subregions. *Hippocampus* **28**, 69–75 (2018).

29. D.N. Barry, I.A. Clark, E.A. Maguire, The relationship between hippocampal subfield volumes and autobiographical memory persistence. *Hippocampus* **31**, 362–374 (2021).

30. P. Zeidman, E.A. Maguire, Anterior hippocampus: the anatomy of perception, imagination and episodic memory. *Nat. Rev. Neurosci.* **17**, 173–182 (2016).

31. M.A. Dalton, P. Zeidman, D.N. Barry, E. Williams, E.A. Maguire, Segmenting subregions of the human hippocampus on structural magnetic resonance image scans: An illustrated tutorial. *Brain Neurosci. Adv.* **1**, 2398212817701448 (2017).

32. P. Zeidman, A. Lutti, E.A. Maguire, Investigating the functions of subregions within anterior hippocampus. *Cortex* **73**, 240–256 (2015).

33. C.J. Hodgetts, *et al.*, Ultra-High-Field fMRI Reveals a Role for the Subiculum in Scene Perceptual Discrimination. *J. Neurosci.* **3**7, 3150–3159 (2017).

34. C.N. Boccara, *et al.*, Grid cells in pre- and parasubiculum. *Nat. Neurosci.* **13**, 987–994 (2010).

35. C. Lever, S. Burton, A. Jeewajee, J. O'Keefe, N. Burgess, Boundary vector cells in the subiculum of the hippocampal formation. *J. Neurosci.* **29**, 9771–9777 (2009).

36. J.P. Shine, J.P. Valdés-Herrera, C. Tempelmann, T. Wolbers, Evidence for allocentric boundary and goal direction information in the human entorhinal cortex and subiculum. *Nat. Commun.* **10**, 4004 (2019).

37. A.J. Dawes, R. Keogh, T. Andrillon, J. Pearson, A cognitive profile of multi-sensory imagery, memory and dreaming in aphantasia. *Sci. Rep.* **10**, 10022 (2020).

38. A. Zeman, M. Dewar, S. Della Sala, Lives without imagery - Congenital aphantasia. *Cortex* **73**, 378–380 (2015).

39. A. Zeman, *et al.*, Phantasia-The psychological significance of lifelong visual imagery vividness extremes. *Cortex* **130**, 426–440 (2020).

40. M. Monzel, A. Vetterlein, M. Reuter, Memory deficits in aphantasics are not restricted to autobiographical memory - Perspectives from the Dual Coding Approach. *J. Neuropsychol.* doi: 10.1111/jnp.12265 (2021).

41. N.W. Watkins, (A)phantasia and severely deficient autobiographical memory: Scientific and personal perspectives. *Cortex* **105**, 41–52 (2018).

42. D.J. Palombo, S. Sheldon, B. Levine, Individual differences in autobiographical memory. *Trends Cogn. Sci. (Regul. Ed.)* **22**, 583–597 (2018).

43. J. Pearson, The human imagination: the cognitive neuroscience of visual mental imagery. *Nat. Rev. Neurosci.* **20**, 624–634 (2019).

44. E.A. Maguire, S.L. Mullally, The hippocampus: a manifesto for change. *J. Exp. Psychol. Gen.* **142**, 1180–1189 (2013).

45. C. McCormick, E. Ciaramelli, F. De Luca, E.A. Maguire, Comparing and contrasting the cognitive effects of hippocampal and ventromedial prefrontal cortex damage: A review of human lesion studies. *Neuroscience* **374**, 295–318 (2018).

46. C. McCormick, C.R. Rosenthal, T.D. Miller, E.A. Maguire, Mind-Wandering in People with Hippocampal Damage. *J. Neurosci.* **38**, 2745–2754 (2018).

47. C. McCormick, C.R. Rosenthal, T.D. Miller, E.A. Maguire, Hippocampal damage increases deontological responses during moral decision making. *J. Neurosci.* **36**, 12157–12167 (2016).

48. C. McCormick, C.R. Rosenthal, T.D. Miller, E.A. Maguire, Deciding what is possible and impossible following hippocampal damage in humans. *Hippocampus* **27**, 303–314 (2017).

49. M.J. Chadwick, H.M. Bonnici, E.A. Maguire, CA3 size predicts the precision of memory recall. *Proc. Natl. Acad. Sci. USA* **111**, 10720–10725 (2014).

50. E.L. Newman, M.E. Hasselmo, CA3 sees the big picture while dentate gyrus splits hairs. *Neuron* **81**, 226–228 (2014).

51. M.T. van Dijk, A.A. Fenton, On how the dentate gyrus contributes to memory discrimination. *Neuron* **98**, 832–845.e5 (2018).

52. S. Baker, *et al.*, The human dentate gyrus plays a necessary role in discriminating new memories. *Curr. Biol.* **26**, 2629–2634 (2016).

53. P. Shah, *et al.*, Mapping the structural and functional network architecture of the medial temporal lobe using 7T MRI. *Hum. Brain Mapp.* **39**, 851–865 (2018).

54. L. Ezama, J.A. Hernández-Cabrera, S. Seoane, E. Pereda, N. Janssen, Functional connectivity of the hippocampus and its subfields in resting-state networks. *Eur. J. Neurosci.* **53**, 3378–3393 (2021).

55. S.L. Ding, Comparative anatomy of the prosubiculum, subiculum, presubiculum, postsubiculum, and parasubiculum in human, monkey, and rodent. *J. Comp. Neurol.* **521**, 4145–4162 (2013).

56. R.A. Epstein, W.E. Parker, A.M. Feiler, Where am I now? Distinct roles for parahippocampal and retrosplenial cortices in place recognition. *J. Neurosci.* **27**, 6141–6149 (2007).

57. M.L. Auger, S.B. Floresco, Prefrontal cortical GABA modulation of spatial reference and working memory. *Int. J. Neuropsychopharmacol.* **18**, (2014) doi:10.1093/ijnp/pyu013.

58. E. Svoboda, M.C. McKinnon, B. Levine, The functional neuroanatomy of autobiographical memory: A meta-analysis. Neuropsychologia 44, 2189–2208 (2006).

59. I.A. Clark, E.A. Maguire, Do questionnaires reflect their purported cognitive functions? *Cognition* **195**, 104114 (2020).

60. D. Brenner, R. Stirnberg, E.D. Pracht, T. Stöcker, ESMRMB 2013, 30th Annual Scientific Meeting, Toulouse, France, 3-5 October: Abstracts, Friday. *Magn Reson Mater Phy* **26**, 151–301 (2013).

61. A.J.W. van der Kouwe, T. Benner, D.H. Salat, B. Fischl, Brain morphometry with multiecho MPRAGE. *Neuroimage* **40**, 559–569 (2008).

62. F.A. Breuer, *et al.*, Controlled aliasing in volumetric parallel imaging (2D CAIPIRINHA). *Magn. Reson. Med.* **55**, 549–556 (2006).

63. J. Hennig, K. Scheffler, Hyperechoes. *Magn. Reson. Med.* **46**, 6–12 (2001).

64. P. Coupé, *et al.*, Robust Rician noise estimation for MR images. *Med Image Anal* **14**, 483–493 (2010).

65. R. Stirnberg, D. Brenner, T. Stöcker, N.J. Shah, Rapid fat suppression for three-dimensional echo planar imaging with minimized specific absorption rate. *Magn. Reson. Med.* **76**, 1517–1523 (2016).

66. P.A. Yushkevich, *et al.*, User-guided 3D active contour segmentation of anatomical structures: significantly improved efficiency and reliability. *Neuroimage* **31**, 1116–1128 (2006).

67. S.L. Ding, G.W. Van Hoesen, Organization and Detailed Parcellation of Human Hippocampal Head and Body Regions Based on a Combined Analysis of Cyto- and Chemoarchitecture. *J. Comp. Neurol.* **523**, 2233–2253 (2015).

68. L.R. Dice, Measures of the Amount of Ecologic Association Between Species. *Ecology* **26**, 297 (1945).

69. H.M. Bonnici, *et al.*, Multi-voxel pattern analysis in human hippocampal subfields. *Front. Hum. Neurosci.* **6**, 290 (2012).

70. D.J. Palombo, *et al.*, KIBRA polymorphism is associated with individual differences in hippocampal subregions: evidence from anatomical segmentation using high-resolution MRI. *J. Neurosci.* **33**, 13088–13093 (2013).

71. A. Krishnan, L.J. Williams, A.R. McIntosh, H. Abdi, Partial Least Squares (PLS) methods for neuroimaging: a tutorial and review. *Neuroimage* **56**, 455–475 (2011).

72. A.R. McIntosh, N.J. Lobaugh, Partial least squares analysis of neuroimaging data: applications and advances. *Neuroimage* **23 Suppl 1**, S250–63 (2004).

73. C. McCormick, M.A. Dalton, P. Zeidman, E.A. Maguire, Characterising the hippocampal response to perception, construction and complexity. *Cortex* **137**, 1–17 (2021).